Srinivasan Vedantham,[1] Devi Thiagarajan,[1] Radha Ananthakrishnan,[1] Lingjie Wang,[1] Rosa Rosario,[1] Yu Shan Zou,[1] Ira Goldberg,[2] Shi Fang Yan,[1] Ann Marie Schmidt,[1] and Ravichandran Ramasamy[1]

Aldose Reductase Drives Hyperacetylation of Egr-1 in Hyperglycemia and Consequent Upregulation of Proinflammatory and Prothrombotic Signals

Sustained increases in glucose flux via the aldose reductase (AR) pathway have been linked to diabetic vascular complications. Previous studies revealed that glucose flux via AR mediates endothelial dysfunction and leads to lesional hemorrhage in diabetic human AR (hAR) expressing mice in an apoE$^{-/-}$ background. Our studies revealed sustained activation of Egr-1 with subsequent induction of its downstream target genes tissue factor (TF) and vascular cell adhesion molecule-1 (VCAM-1) in diabetic apoE$^{-/-}$hAR mice aortas and in high glucose–treated primary murine aortic endothelial cells expressing hAR. Furthermore, we observed that flux via AR impaired NAD$^+$ homeostasis and reduced activity of NAD$^+$-dependent deacetylase Sirt-1 leading to acetylation and prolonged expression of Egr-1 in hyperglycemic conditions. In conclusion, our data demonstrate a novel mechanism by which glucose flux via AR triggers activation, acetylation, and prolonged expression of Egr-1 leading to proinflammatory and prothrombotic responses in diabetic atherosclerosis.

Diabetes 2014;63:761–774 | DOI: 10.2337/db13-0032

Posttranslational modification (PTM) of histones via deacetylation, mediated by a family of histone deacetylases, was initially identified as a mechanism to silence gene transcription (1,2). In addition, it is well established that acetylation and deacetylation of nonhistone proteins are common PTMs found across the cytosol, nucleus, mitochondria, and endoplasmic reticulum (3), including enzymes involved in intermediary metabolism (4,5). These findings support a broader role for acetylation beyond the nucleus. Sirtuins are NAD$^+$-dependent enzymes, well-known to deacetylate proteins and enzymes (6), including the proteins that play important roles in metabolism (7). Sirtuins have been shown to regulate various transcription factors such as p53 (8,9), forkhead box class O (10), peroxisome proliferator–activated receptor-γ (11), p65 subunit of nuclear factor-κB (NF-κB) (12,13), and peroxisome proliferator–activated receptor-γ coactivator 1-α (14). Sirt-1 has been shown to have atheroprotective effects, and inhibition of its activity using pharmacological agents or genetic deletion induces arterial thrombus formation (13).

[1]Diabetes Research Program, Department of Medicine, New York University Langone Medical Center, New York, NY
[2]Division of Preventive Medicine and Nutrition, Columbia University Medical Center, New York, NY

Corresponding author: Ravichandran Ramasamy, ramasr02@nyumc.org.

Received 11 January 2013 and accepted 3 October 2013.

This article contains Supplementary Data online at http://diabetes.diabetesjournals.org/lookup/suppl/doi:10.2337/db13-0032/-/DC1.

S.V., D.T., and R.A. contributed equally to this work.

See accompanying commentary, p. 402.

Expression of human aldose reductase (hAR) in an atherosclerosis-vulnerable LDL receptor knockout mouse ($Ldlr^{-/-}$) background increased atherosclerosis in diabetic mice (15). Subsequent studies revealed aldose reductase (AR)-mediated defects in vasorelaxation, endothelial function, and lesional hemorrhage in hAR-overexpressing mice with streptozotocin-induced diabetes in an apolipoprotein (apo)$E^{-/-}$ background (16). Flux of glucose via the AR pathway consumes NAD^+ by the action of the sorbitol dehydrogenase (SDH) to generate fructose. As a consequence, increased flux of glucose via this pathway in hyperglycemia leads to a decrease in NAD^+-to-NADH ratio (17). In this study, we investigated whether flux via AR causes proinflammatory and prothrombotic signaling via NAD^+ reduction and subsequent inhibition of Sirt-1–dependent deacetylation of Egr-1 ("immediate early response gene"). Our data demonstrate a novel mechanism linking glucose metabolism to increased inflammatory and prothrombotic signaling in diabetic atherosclerosis via PTM of Egr-1.

RESEARCH DESIGN AND METHODS

All animal studies were performed with the approval of the Institutional Animal Care and Use Committee at New York University. The hAR mice and apo$E^{-/-}$hAR mice, both backcrossed >10 generations into C57BL/6, were characterized and rendered diabetic with streptozotocin as previously described (18). Details of the treatment of diabetic mice with inhibitors of AR are described in the supplement.

Cell Culture

Murine aortic endothelial cells (MAECs) were established from mouse aortas as previously described (19), while human aortic endothelial cells (HAECs) were from a commercial source (Cell Applications). Studies on these cultured cells included treatment with the AR inhibitor (ARI) zopolrestat (200 μmol/L), SDH inhibitor (SDI) CP-470711 (200 nmol/L), nicotinamide mononucleotide (NMN) (500 μmol/L), the sirtuin inhibitor sirtinol (20 nmol/L), DMSO, or Sirt activator SRT1720 (10 μmol/L). Endothelial cells were transfected overnight using an adenoviral vector overexpressing hAR or GFP (Vector Biolabs) in serum-free medium.

Generation of Egr-1 Mutants, In Vitro Acetylation, and Deacetylation Assays

The mutant Egr-1 was generated as previously described (20). Briefly, an *Eco*RV-*Sma*I full-length, flag-tagged Egr-1 from pCMVFLAG-Egr-1 was inserted into the *Eco*RV site in pcDNA3 to generate pcDNA3-Egr-1. Egr-1 has acetylation sites 422–425 corresponding to the consensus sequence KDKK. Site directed mutants EgrM1 (ADKK), EgrM2 (KDAK) and EgrM3 (KDKA) were generated using the following primers: EGRM1 (atccatttaagacagGCGgacaagaaagcagacaaaagtgtggtg), EGRM2 (atccatttaagacagGCggacGCGGCAgcagacaaaagtgtggtg), and EGRM3 (atccatttaagacagaaggacGCGGCAgcagacaaaagtgtggtg)—using the QuikChange Multi Site-Directed Mutagenesis kit (Stratagene, San Diego, CA). The Egr-1 mutants (EGRM1, EGRM2, And EGRM3) generated were sequenced and confirmed for the appropriate mutations and further transformed in *Escherichia coli* and purified using Ni-NTA column. The purified Egr-1 and the mutants were used as substrate for in vitro acetylation studies.

The in vitro acetylation studies were performed as previously described (9). Briefly, 1 μg purified Egr-1 protein was added to the 30 μL assay mixture consisting of 50 mmol/L HEPES (pH 8.0), 10% glycerol, 1 mmol/L dithiothreitol, 1 mmol/L phenylmethylsulfonyl fluoride, 10 mmol/L sodium butyrate, 0.2 mCi [14C] acetyl-CoA (4 mCi/mmol; Perkin Elmer), 10 mmol/L cold acetyl-coA, and 100 ng recombinant p300 protein (Activ Motif) for 1 h at 30°C. For electrophoretic mobility shift assays, the reaction mixture was subjected to SDS-PAGE gels and developed either by autoradiography or by Western blot using acetyllysine antibody (Millipore).

For the in vitro deacetylation studies (21), the assay mixture containing the acetylated Egr-1 was subjected to a deacetylation reaction containing an assay buffer (50 mmol/L Tris-HCl, pH 8.0; 4 mmol/L $MgCl_2$; and 0.2 mmol/L dithiothreitol), 300 ng recombinant Sirt-1 protein, and 50 μmol/L NAD^+. The assay mixture was incubated for 1 h at 30°C and was subjected to SDS-PAGE gel visualized either through autoradiography or through Western blot by acetyllysine antibody.

Chromatin Immunoprecipitation

Chromatin immunoprecipitation (ChIP) was performed using the ChIP-IT kit (Activ Motif). Briefly, MAECs were cross-linked with 1% formaldehyde in PBS for 15 min at room temperature. Samples were processed per instructions provided by the manufacturer to obtain chromatin. The chromatin was initially precleared using protein-G beads and subsequently treated with Egr-1 antibody (Santa Cruz Biotechnology) at a concentration of 1:200 for immunoprecipitation overnight. The immunoprecipitated ChIP product was washed, reverse cross-linked, treated with proteinase K, and eluted to get the ChIP-enriched DNA. Simultaneously, IgG was used as a negative control to check the efficiency of the ChIP experiment. ChIP-enriched DNA (25 ng) was used to perform PCR for the tissue factor (TF) promoter using the following primers: forward, 5′ CATCCCTTG CAGGGTCCCGGAGTT 3′; reverse, 5′ GGGGTGCGGG AGCTCGCAGTC 3′. The PCR products were run on a 2% agarose gel, and the amplicons were visualized using ultraviolet light.

Standard methods for studies involving RNA silencing, Western blotting, immunoprecipitation, quantitative real-time PCR, immunohistochemistry, and transient transfection of MAEC or HAECs with hAR or green

fluorescent protein were followed (16). Assays for murine plasma TF (MyBiosource,), NAD^+/NADH measurements (Biovision), luciferase reporter, Sirt-1 (Sigma Aldrich), and nicotinamide phosphoribosyl transferase (NAMPT) (Cyclex) activities were performed per the manufacturer's instructions.

Statistical Analysis

All data are reported as means ± SD unless otherwise noted. Data were analyzed by one-way ANOVA using commercially available software (version 18; SPSS). Probability values ≤0.05 were considered statistically significant.

RESULTS

Expression of Egr-1 in Diabetic ApoE$^{-/-}$hAR Mice Aorta

We previously reported that transgenic expression of human-relevant levels of AR accelerated vascular dysfunction, atherogenesis, lesional hemorrhage, and inflammation in diabetic apoE$^{-/-}$hAR mice (16). In this study, we sought to test the hypothesis that expression of hAR in these mice upregulated Egr-1, a key transcription factor linked to regulation of inflammation and prothrombotic responses. Aortas collected from 14-week-old diabetic apoE$^{-/-}$hAR mice demonstrated a threefold higher gene expression of Egr-1 compared with nondiabetic apoE$^{-/-}$hAR aortas ($P < 0.05$) (Fig. 1*A*). Similarly, there was a significant rise in Egr-1 protein expression in diabetic apoE$^{-/-}$hAR aorta compared with the nondiabetic apoE$^{-/-}$hAR group ($P < 0.05$) (Fig. 1*B*). Aortas obtained from nondiabetic wild-type (WT) and hAR-overexpressing mice at comparable age showed no significant changes in the expression level of Egr-1 (Supplementary Fig. 1*A*) Expression of Egr-1 in the aorta was observed from 10 weeks of diabetes (Supplementary Fig. 1*B*).

Immunohistochemistry of apoE$^{-/-}$hAR aortic root revealed significant localization of Egr-1 to the endothelial lining of the aorta in the 14-week diabetic group compared with the nondiabetic group (Fig. 1*C*). Quantitation of Egr-1 and AR signals in the endothelial lining indicate that expression of Egr-1–AR colocalized signal is increased in diabetic vs. nondiabetic apoE$^{-/-}$hAR mice (Fig. 1*D–F*). We previously demonstrated the role of ARI zopolrestat in reducing atherosclerotic lesions in diabetic apoE/-hAR mouse aortas. We sought to determine whether administration of ARIs modulated expression and action of Egr-1 in the vasculature. Expression of Egr-1 protein was reduced in the diabetic apoE$^{-/-}$hAR mice aorta treated with zopolrestat versus vehicle (Fig. 1*G*) ($P < 0.05$).

High Glucose–Induced Egr-1 Expression in MAECs: Effect of hAR

Primary MAECs cultured from the aortas of hAR mice treated with high glucose (25 mmol/L D-glucose) for 24 h showed a significant increase in nuclear Egr-1 protein expression compared with cells cultured in physiologic levels of glucose (5 mmol/L D-glucose) (Fig. 2*A*) ($P < 0.05$). Reduction of hAR expression by small interfering RNA (siRNA) for AR (Fig. 2*A*) or activity by ARI zopolrestat (Fig. 2*B*) showed a significant decrease ($P < 0.05$) in expression of nuclear Egr-1.

MAECs subjected to high glucose revealed a time-dependent upregulation of Egr-1 mRNA expression. The WT cells showed increased expression of Egr-1 mRNA at 30 min that peaked at 2 h (fivefold compared with 0 h, $P < 0.05$) and then tapered down to levels comparable with the 0-h time point. In contrast, the cells expressing hAR showed a significant rise in Egr-1 expression at 2 h (compared with control cells at similar time point, $P < 0.05$) that was sustained until 8 h and then subsequently tapered down by 24 h but was fivefold higher compared with the WT cells (Fig. 2*C*) ($P < 0.05$). A similar observation was made when the cells were probed for Egr-1 protein expression at these time points (Fig. 2*D*).To further validate that these changes in Egr-1 expression were due to transcriptional regulation, we tested Egr-1 promoter activity. Egr-1 promoter luciferase reporter activity was significantly greater in hAR-overexpressing cells (9.75 ± 1.76 RLU) compared with the control WT cells grown in high glucose (3.54 ± 1.46 RLU), $P < 0.05$ (Fig. 2*E*). For determination of whether flux via AR and SDH (the latter the second enzyme in the pathway that consumes NAD^+) is required for Egr-1 regulation in high glucose, we incubated MAECs in high glucose alone or in the presence of ARI or SDI. A significant increase in total Egr-1 protein expression was noted compared with the low glucose (5.5 mmol/L)-treated cells; consistent with key roles for AR and SDH, MAECs treated with either ARI or SDI demonstrated significantly reduced expression of Egr-1 in the presence of high glucose versus untreated cells (Fig. 2*F*).

Acetylation of Egr-1 Is Required for Its Sustained Expression

Since stabilization and expression of Egr-1 occurs through its acetylation by CBP/p300 at a CBP/p300 consensus sequence (KDKK) (20), we asked whether the difference in expression patterns of Egr-1 in high glucose in WT versus hAR MAECs was dependent, at least in part, on differences in PTM, i.e., acetylation. To test this, we performed immunoprecipitation experiments with antibody recognizing acetyllysine followed by Western blotting with antibody to Egr-1 in high or low glucose–treated MAECs. Upon 24 h treatment with high glucose, significantly greater degrees of acetylated Egr-1 protein were immunoprecipitated from hAR versus control MAECs (Fig. 3*A*). Time course experiments revealed that the first evidence of acetylated Egr-1 protein in high glucose occurred after 2 h incubation in MAECs (Fig. 3*B*). Consistent with key roles for AR and SDH in mediating acetylation of Egr-1, treatment of MAECs with ARI or SDI resulted in decreased acetylated Egr-1 immunoprecipitated with antibody recognizing acetyllysine from high glucose–treated cells (Fig. 3*A*). We next sought to test whether analogous findings were evident in HAECs.

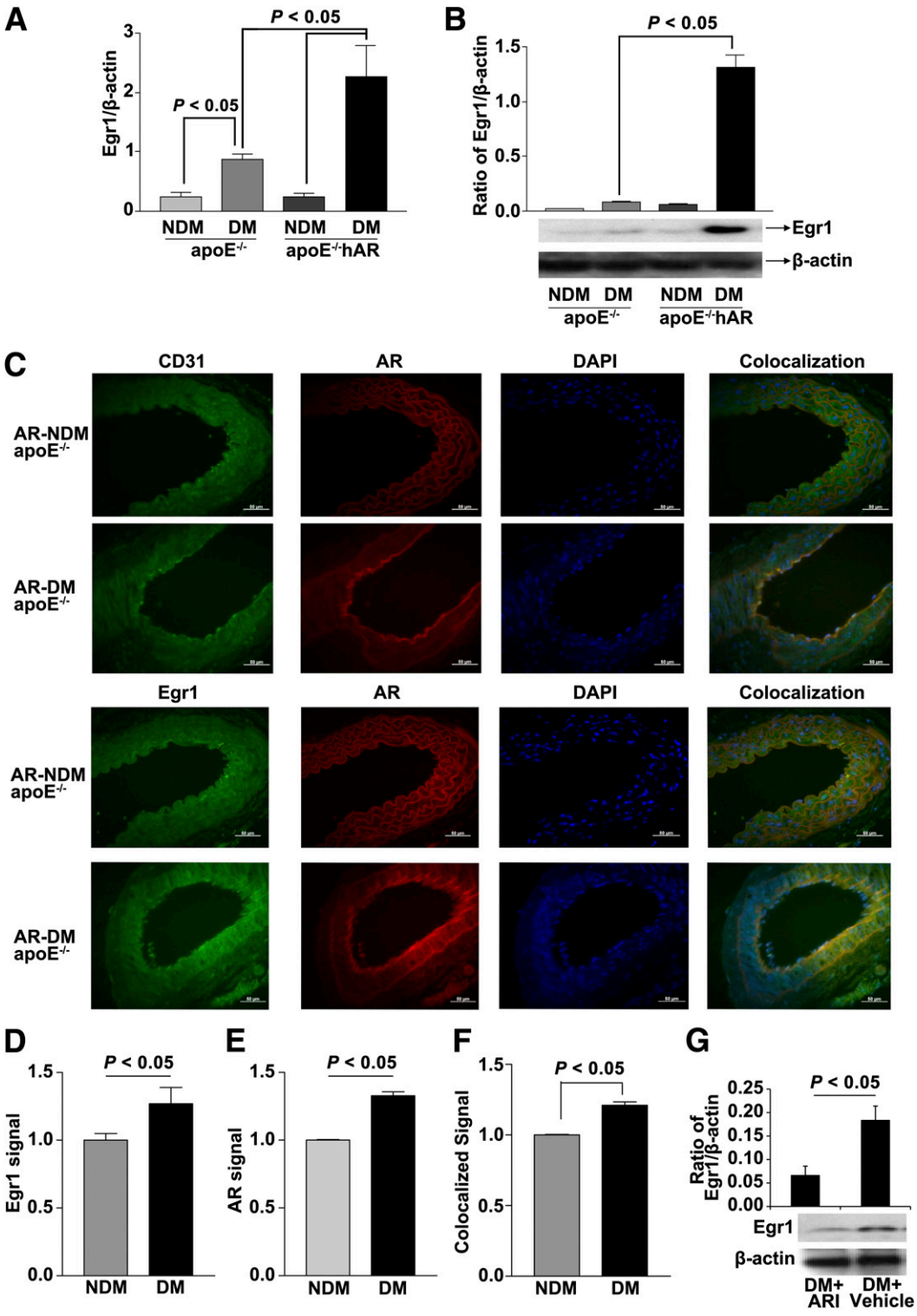

Figure 1—Expression of Egr-1 in aorta collected from nondiabetic (NDM) apoE$^{-/-}$ and 14-week diabetic (DM) apoE$^{-/-}$hAR mice. *A*: mRNA expression of Egr-1 in aorta from apoE$^{-/-}$ and apoE$^{-/-}$hAR mice with and without diabetes ($N \geq 3$, $P < 0.05$). *B*: Protein expression of Egr-1 from DM and NDM apoE$^{-/-}$ and apoE/$^{-}$hAR mice aorta ($N = 3$; $P < 0.05$). *C*: Representative immunohistochemistry of the aortic root from apoE$^{-/-}$hAR mice with diabetes demonstrating colocalization of Egr-1 and AR in the endothelial cells (using anti-CD31 IgG). *D*: Pixel intensities of IHC sections of aorta from NDM and DM apoE/$^{-}$hAR mice stained with Egr-1 or AR antibody (*E*). *F*: Colocalized Egr-1 and AR were then quantitated using the Axiovision LE 4.8.2 program. *G*: Expression of Egr-1 protein in the aortic tissues of DM apoE$^{-/-}$hAR mice treated with ARI or vehicle ($N = 3$; $P < 0.05$).

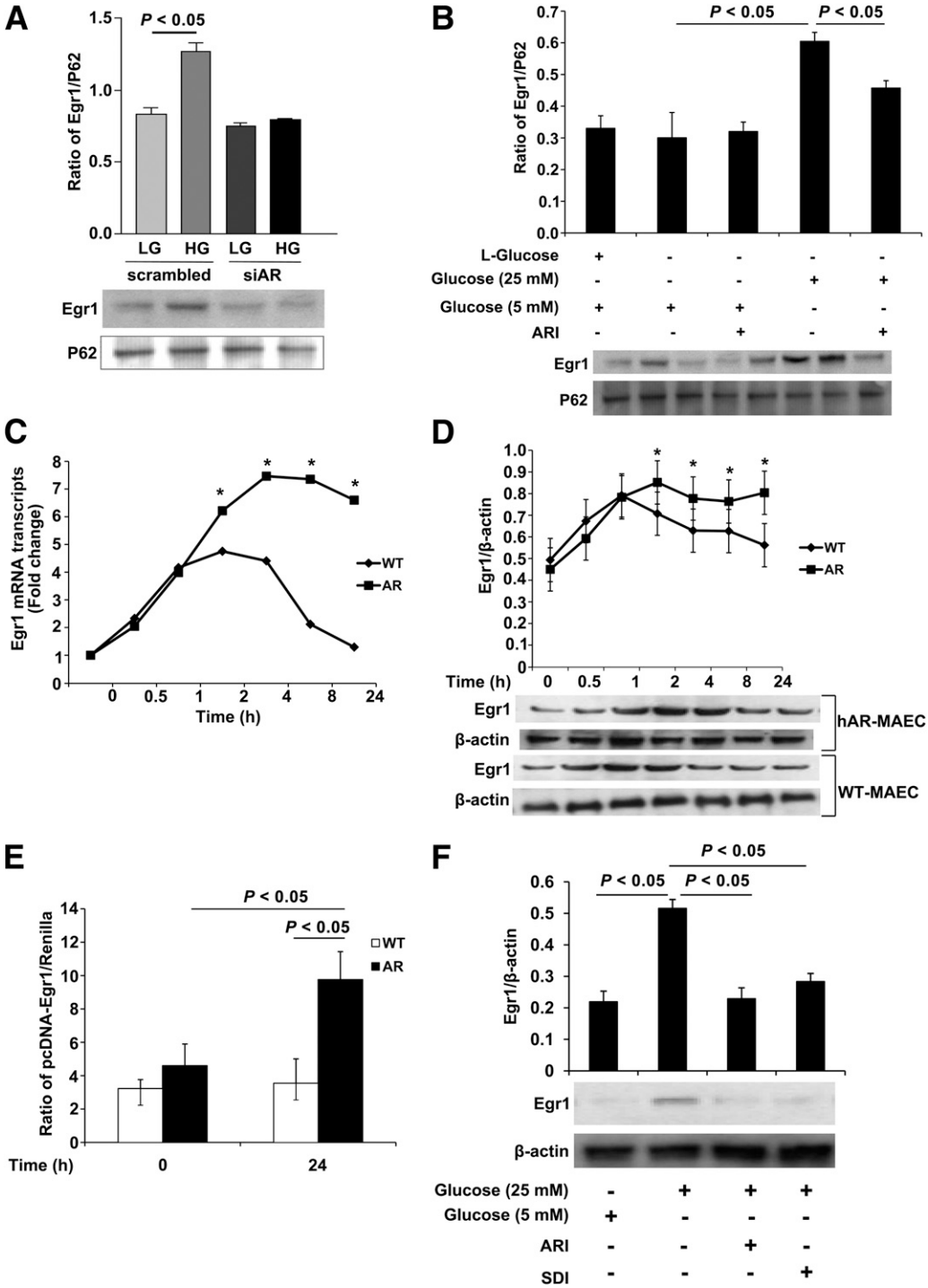

Figure 2— Expression of Egr-1 in primary aortic endothelial cells. *A*: Protein expression of Egr-1 in MAECs overexpressing hAR. Cells were either silenced with siRNA for hAR or treated with a scrambled siRNA and further exposed to physiological levels of glucose (5 mmol/L) or high glucose (25 mmol/L) for 24 h. Subcellular fractionation was performed to collect the nuclear fractions and probed for Egr-1 using Western blot. Results are expressed as ratio of Egr-1 to P62 ($N = 3$; $P < 0.05$). *B*: Protein expression of Egr-1 by Western blot in nuclear fractions of MAECs treated with 5.5 mmol/L glucose or high glucose along with an ARI. MAECs treated with L-glucose were used as osmotic control. Results were expressed as ratio of Egr-1 to P62 from at least three different cell types from the same treatments ($P < 0.05$). *C*: mRNA transcript expression of Egr-1 in WT MAECs or MAECs overexpressing hAR treated with high glucose at various time points. The results were expressed as fold change compared with the 0-h time point (*$P < 0.05$). *D*: Protein expression of Egr-1 by Western blot in MAECs overexpressing hAR treated with high glucose at various time points. Results expressed as ratio of Egr-1 to β-actin from at least three independent experiments (*$P < 0.05$). *E*: Promoter activity of Egr-1 using a luciferase assay in MAECs isolated from WT and hAR-overexpressing mice. Cells were treated with high glucose for 24 h, and luciferase activity was measured. Results are expressed as the ratio of pcEgr-1-lucA to renilla from at least three independent experiments. *F*: Protein expression of Egr-1 in HAECs treated with high glucose and 5.5 mmol/L glucose along with ARI and SDI for 24-h. Blot is a representative figure from at least three independent experiments. HG, high glucose; LG, low glucose; siAR, siRNA for AR.

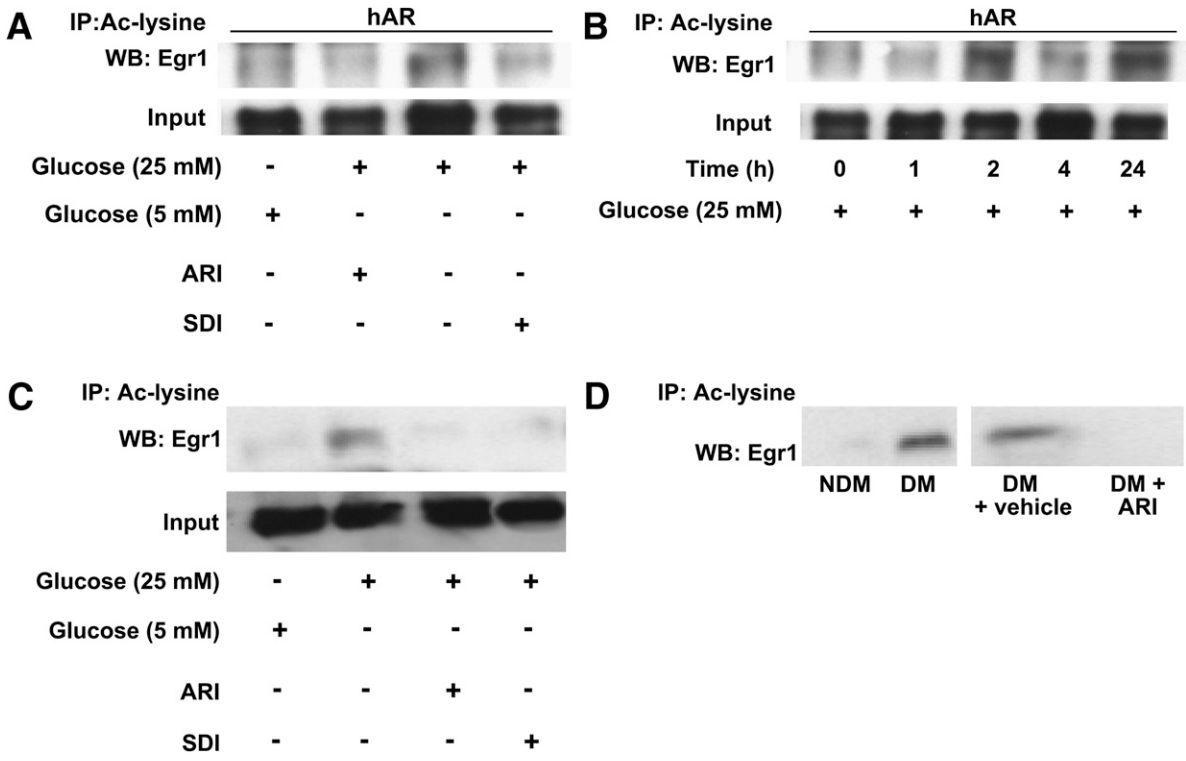

Figure 3—Measurement of acetylated Egr-1 in primary MAECs and aortic tissues from apoE$^{-/-}$hAR mice using immunoprecipitation (IP) with anti-acetyllysine antibody followed by Western blotting for Egr-1. *A*: Expression of acetylated Egr-1 in MAECs overexpressing hAR in cells treated with high glucose and 5.5 mmol/L glucose for 24 h along with ARI and SDI. *B*: Time-dependent expression of acetylated Egr-1 in MAECs treated with high glucose. *C*: Expression of acetylated Egr-1 in HAECs treated with 5.5 mmol/L and high glucose along with ARI and SDI. *D*: Acetylated Egr-1 expression in aorta isolated from 14-week diabetic (DM) and nondiabetic (NDM) apoE$^{-/-}$hAR mice and in DM mice treated with ARI for 14 weeks. Results are representative of at least three independent experiments. Ac-lysine, acetyllysine; WB, Western blot.

HAECs treated with high glucose for 24 h showed significantly more immunoprecipitated acetylated Egr-1 expression versus the low-glucose condition. Presence of ARI or SDI in high-glucose medium markedly reduced acetylated Egr-1 expression to the levels observed in low glucose–treated HAECs (Fig. 3*C*). Consistent with in vitro cell culture data, significant acetylation of Egr-1 was observed in streptozotocin-treated apoE$^{-/-}$hAR mice aorta compared with nondiabetic controls in an AR-dependent manner, as treatment of diabetic apoE$^{-/-}$hAR mice with ARI reduced acetylation of Egr-1 in the aorta versus vehicle treatment (Fig. 3*D*).

Polyol Flux Through AR Decreases NAMPT Activity, NAD+ Synthesis, and Sirt-1 Activity

Flux of glucose via the AR pathway has been demonstrated to cause reductions in the ratio of NAD^+ to NADH. We hypothesized that reductions in the NAD^+-to-NADH ratio, due to AR flux, decreases Sirt-1 activity, which, in turn, would expose Egr-1 for acetylation by the histone acetyltransferases (HATs) such as CBP/p300. To address this question, we assessed expression of Sirt-1 protein in MAECs from hAR-overexpressing mice. Time-dependent exposure of the cells to high glucose revealed a significant decrease in the total (Fig. 4*A*) and nuclear (Fig. 4*B*) expression of Sirt-1 by 24 h. Prolonging the incubation time to 48 h under high glucose did not lead to additional decreases in Sirt-1 expression of MAECs in hAR-overexpressing mice (data not shown). Treatment with an ARI restored levels of Sirt-1 to those observed in the low glucose–treated cells. Similarly, treatment of MAECs with either resveratrol or NMN, which improves the Sirt-1 activity, resulted in increased expression of Sirt-1 in the nucleus (Fig. 4*B*). We next measured Sirt-1 activity; cells treated with high glucose showed a significant 40% decrease in Sirt-1 activity compared with low glucose–treated cells ($P < 0.05$) (Fig. 4*C*). However, the Sirt-1 activity was restored by almost threefold (compared with high-glucose treatment) when the cells were exposed to NMN (an activator of NAD synthesis and, subsequently, Sirt-1 activity) and was improved when cells were treated with either ARI or SDI ($P < 0.05$) (Fig. 4*C*). Aortic tissues isolated from 14-week diabetic apoE$^{-/-}$hAR mice with streptozotocin treatment showed a 45% decrease in Sirt-1 activity compared with the nondiabetic apoE$^{-/-}$hAR aorta ($P < 0.05$) (Fig. 4*D*). In vivo, treatment of the diabetic mice with ARI for the entire duration of diabetes (14 weeks) normalized the

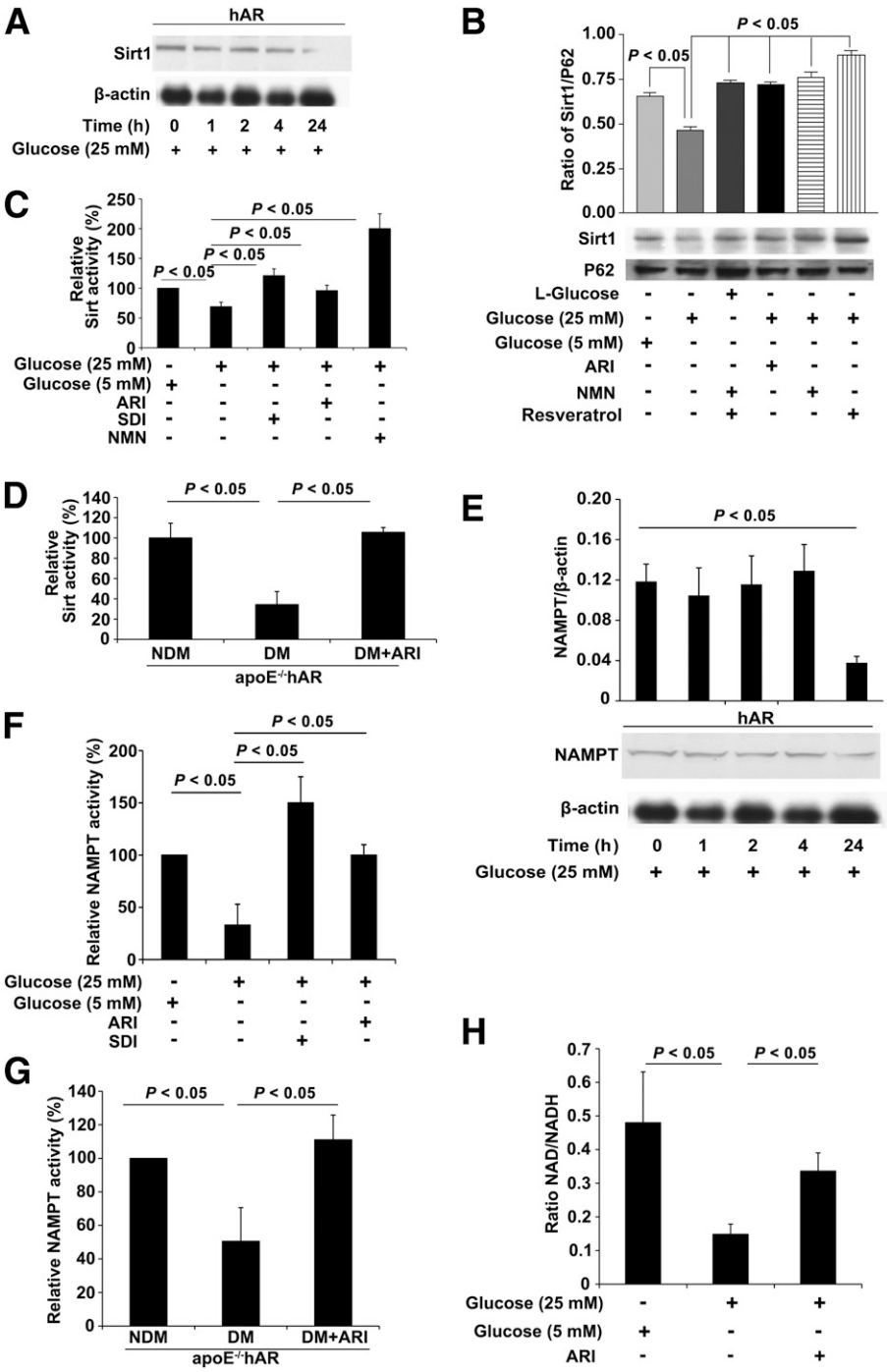

Figure 4—Sirt-1, NAMPT expression and activity, and NAD^+-to-NADH ratio measured in primary aortic endothelial cells and aorta tissues. *A*: Protein expression of Sirt-1 at various time points of treatment with high glucose in MAECs overexpressing hAR. Results are expressed as ratio of Sirt-1 expression to β-actin. *B*: Expression of Sirt-1 in the nuclear fractions of MAECs treated with high and 5.5 mmol/L glucose along with ARI, NMN, and resveratrol for 24 h. Results are expressed as ratio of Sirt-1 to P62. *C*: Sirt-1 activity measured in MAECs treated with 5.5 mmol/L and high glucose along with ARI, SDI, and NMN. Results are expressed as relative percent activity compared with cells treated with 5.5 mmol/L glucose. *D*: Sirt-1 activity in aortas isolated from apoE$^{-/-}$hAR mice with (DM) and without diabetes (NDM) and diabetic mice treated with ARI (DM+ARI). Results are expressed as relative Sirt-1 activity compared with NDM. ($N \geq 4$; $P < 0.05$.) *E*: Protein expression of NAMPT in MAECs overexpressing hAR upon treatment with high glucose for various time points. *F*: NAMPT activity measured in MAECs overexpressing hAR upon treatment with 5.5 mmol/L and high glucose along with ARI and SDI. Results are expressed as relative percent activity compared with the 0-h treatment with high glucose or with 5.5 mmol/L glucose–treated cells, respectively. *G*: NAMPT activity measured in aorta isolated from 14-week DM, NDM, or ARI-treated apoE$^{-/-}$hAR mice. Results are expressed as relative percent activity compared with NDM mice ($N \geq 4$; $P < 0.05$). *H*: Measurement of NAD^+-to-NADH ratio in MAECs overexpressing hAR, treated with 5.5 mmol/L, 25 mmol/L, and 25 mmol/L glucose along with ARI. All experiments are representative of at least $N = 3$ replicates.

Sirt-1 activity to levels comparable with those of the nondiabetic apoE$^{-/-}$hAR mice (Fig. 4*D*).

To determine whether the availability of NAD+ was limiting or if its synthesis was impacted, we measured the expression of NAMPT, the rate-limiting enzyme in the NAD$^+$ salvage pathway. MAECs treated with high glucose for the indicated time points showed a significant reduction in NAMPT protein expression by 24 h ($P < 0.05$) (Fig. 4*E*). In HAECs, the NAMPT activity was 60% less in cells treated with high glucose in comparison with the low glucose–treated cells ($P < 0.05$) (Fig. 4*F*). Pharmacological inhibition of AR resulted in a significant improvement in NAMPT activity, which was comparable with that of normal glucose–treated HAECs (Fig. 4*F*). Diabetic apoE$^{-/-}$hAR mice demonstrated a 55% decrease in NAMPT activity in the aorta compared with nondiabetic apoE$^{-/-}$hAR mice, which was fully restored by treatment of the diabetic mice with ARI for 14 weeks (Fig. 4*G*).

Next, we measured the NAD$^+$-to-NADH ratio in MAECs, as this was our chief hypothesis; i.e., high glucose–mediated flux via AR and SDH would consume NAD$^+$. NAD$^+$ and NADH were measured as picomoles/million cells, and the ratio was found to be at least three times lower in high glucose–treated MAECs compared with the normal glucose–treated MAECs ($P < 0.05$) (Fig. 4*H*). We hypothesized that acetylation of Egr-1 is an end result of decreased Sirt-1 activity driven by reduced NAD$^+$-to-NADH ratio. To prove this, we first sought to determine whether treatment of cells with high glucose had any effect on the HATs; hence, we measured the total HAT activity in the MAECs overexpressing hAR. No significant differences in HAT activity were observed between the high glucose– and the low glucose–treated cells, thereby implying that acetylation is tightly regulated by the availability of NAD+, which directly impacts Sirt-1 activity. To test this concept, we measured the degree of acetylated Egr-1 in hAR overexpressing MAECs exposed to high glucose or to high glucose with NMN (the latter will restore NAD$^+$). Indeed, we observed decreased acetylation of Egr-1 in MAECs treated with high glucose plus NMN (Fig. 5*A*). Similarly, when cells in high-glucose medium were treated with a sirtuin inhibitor (sirtinol), we observed increased acetylation of Egr-1, thereby confirming that Sirt-1 is required for deacetylation of Egr-1 (Fig. 5*A*). An additional study was performed to determine whether inhibition of NAMPT, which affects NAD$^+$ synthesis, would modulate Egr-1 acetylation. Treatment of MAECs with FK866, a specific inhibitor of NAMPT, in MAECs grown in low glucose resulted in increased acetylation compared with untreated cells (Supplementary Fig. 3). Furthermore, treatment of HAECs with SRT1720 (an activator of Sirt-1) or overexpression of Sirt in HAECs in the high-glucose condition revealed reduced acetylation of Egr-1 (Supplementary Fig. 4).

To determine whether the consensus sequence KDKK within Egr-1, a known site for acetylation by CBP/p300, is a potential site for Sirt-1 action, we generated triple mutants of the Egr-1 protein; we mutated three of these K (lysine) residues to alanine (K419, K421, and K422) and performed in vitro acetylation assays in the WT and the mutant protein using recombinant p300. The acetylated Egr-1 was then subjected to in vitro deacetylation using recombinant Sirt-1 in the presence or absence of NAD$^+$. Sirt-1 convincingly deacetylated the WT Egr-1 protein in the presence of NAD$^+$, which was not observed in the reaction mixture without NAD$^+$ (Fig. 5*B*). We generated single and double mutants of the Egr-1 and noticed appreciable acetylation in the WT single mutant

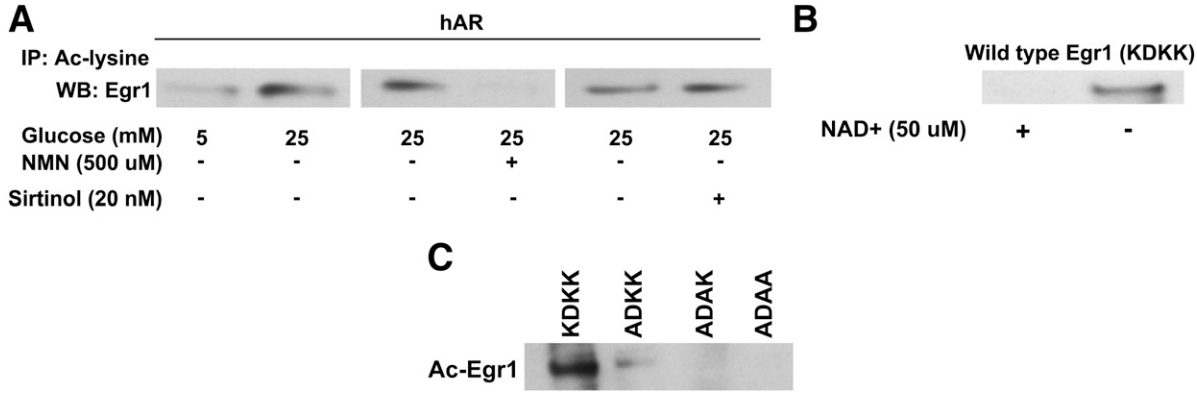

Figure 5—Expression of acetylated Egr-1 in MAECs overexpressing hAR (*A*) treated with 5.5 mmol/L and high glucose along with sirtinol (sirtuin inhibitor) or NMN (sirtuin activator) for 24 h. *B*: In vitro deacetylation assay was performed with WT Egr-1 (preserved KDKK sequence/p300 binding site) as substrate and recombinant Sirt-1 as the enzyme with and without NAD$^+$. The figures represent acetylation of Egr-1 after the deacetylation assay, subjected to SDS-PAGE gel and Western blotting using anti–acetyllysine antibody. *C*: WT Egr-1 (KDKK) and Egr-1 mutants (ADKK, ADAK, and ADAA) were subjected to in vitro acetylation using recombinant p300, and the figure represents the acetylated Egr-1 after the acetylation assay mixture was subjected to SDS-PAGE gel and probed with anti-acetyllysine antibody. Ac-lysine, acetyllysine; IP, immunoprecipitation, WB, Western blot.

but not in the double and the triple mutants (Fig. 5*C*). Thus, this study shows clear evidence for deacetylation of Egr-1 by Sirt-1 and, indeed, that NAD^+ is critical for the catalytic activity of Sirt-1 in deacetylating Egr-1.

AR-Mediated Modulation of Egr-1 Expression Results in Proinflammatory and Prothrombotic Signals in Endothelial Cells

We next sought to test the downstream consequences of overexpression of hAR in MAECS in the presence of Egr-1 silencing. We observed that hAR MAECs grown in high glucose revealed increased expression of vascular cell adhesion molecule-1 (VCAM-1) protein compared with cells grown in low glucose. Upregulation of VCAM-1 in high glucose was dependent at least in part on Egr-1, as siRNA silencing of Egr-1 resulted in decreased expression of VCAM-1 in high glucose (Fig. 6*A*), which was comparable with that of cells treated with normal glucose conditions. Further, expression of TF, a well-known target gene of Egr-1 and a prominent prothrombotic molecule, was significantly higher in hAR cells exposed to high-glucose treatment compared with low-glucose treatment (Fig. 6*B* and *C*). siRNA-mediated reduction of hAR (Fig. 6*B*), blockade of AR activity by ARI (Fig. 6*C*), or silencing of Egr-1 by siRNAs (Fig. 6*D*) each resulted in a significant decrease in TF expression compared with the high glucose–treated conditions. We performed ChIP experiments to study the promoter occupancy of Egr-1 in the TF gene. ChIP studies revealed increased occupancy of Egr-1 in MAECs expressing hAR versus WT cells exposed to high glucose for 24 h (Fig. 6*E*). Finally, we collected plasma from nondiabetic or diabetic $apoE^{-/-}$hAR mice and found increased TF expression in the diabetic (129.35 ± 3.05, $P < 0.05$) compared with the nondiabetic (112.37 ± 4.47) mice (Fig. 6*F*), which was significantly reduced by treatment of the diabetic mice with ARI (115.6 ± 5.02, $P < 0.05$) (Fig. 6*F*).

DISCUSSION

High-glucose flux via the AR pathway leads to altered metabolism of glucose and vascular perturbation (22). Our earlier studies demonstrated that hAR expression in $apoE^{-/-}$ mice, both globally and particularly in endothelial cells, contributes to accelerated diabetic atherosclerosis and that treatment with an ARI reduced atherosclerosis in these diabetic mice (16). In this study, we sought to identify the discrete molecular mechanisms driving the impact of AR in diabetic atherosclerosis. In this study, we report that excess flux of glucose via AR *1*) compromised the NAMPT-mediated NAD^+ synthesis due to excess demand oversupply; *2*) decreased NAD^+, which affects the biological action of Sirt-1 and NAD^+-dependent deacetylases, which in turn triggers acetylation and prolonged expression of Egr-1 leading to proinflammatory and prothrombotic responses; and *3*) that a competitive inhibitor of AR, zopolrestat, normalizes the NAD^+ levels by improving the NAMPT and Sirt-1 activity with subsequent blockade of acetylated Egr-1 expression, thereby prohibiting signals for inflammation and thrombus formation. This study is the first to definitively demonstrate, both in vivo and in primary MAECs and HAECs, that defects in NAD^+ metabolism due to flux via AR have a pathological impact on endothelial activation in diabetes.

AR pathway flux–driven changes in ratio of free cytosolic NADH to NAD^+ as a critical mediator of diabetic vascular complications have been proposed (17). Excess flux of glucose through AR impacts other metabolic pathways such as glycolysis, oxidative stress, intracellular nonenzymatic glycation, and protein kinase C activation (23–27). Here, we draw attention to the link between AR flux and the NAD^+ salvage pathway. Studies have highlighted emerging roles of NAD^+ as a key signaling component in transcriptional regulation, aging, and other diseases (28). In addition to its function in various biological processes, NAD^+ acts as substrate for various enzymes including the NAD^+-dependent sirtuin family of deacetylases (7,28). In this study, we show that Egr-1 is an important substrate for Sirt-1 in the endothelial vasculature. In vitro, at the transcript level, Egr-1 upregulation is seen within 30 min of high-glucose exposure of MAECs. However Sirt activity changes are seen only at 24 h. The initial Egr-1 upregulation observed could be due to the changes at the transcriptional level, whereas the sustained Egr-1 upregulation is likely due to PTMs mediated by the decrease in Sirt activity at 24 h. Inhibition of Sirt-1 activity maintains Egr-1 in an acetylated state that signals prothrombotic and proinflammatory events in the vascular bed. Taken together, both NAMPT-mediated NAD^+ biosynthesis and Sirt-1 play critical roles in regulating such processes as metabolism, stress responses, and cellular differentiation in response to various stimuli such as fasting and caloric restriction (28). A recent study showed decreased NAD^+ and NAMPT levels in multiple organs during aging, along with glucose intolerance in high-fat diet–fed mice (29). In this context, our study highlights the specific effect of glucose flux via the AR pathway on the availability of NAD^+. The effect of continuous flux through the AR pathway leads to alteration of the NAD^+-to-NADH ratio, thereby compromising the NAMPT-mediated NAD^+ biosynthesis. Under these circumstances, the NAMPT activity is compromised either through increased demand for supply of NAD^+ or through a feedback inhibition of NADH on the NAMPT activity. Although in our study we observed a trend in change in NAMPT activity by 2 h (upon exposure to excess glucose), it was only at the 8-h and 24-h time points that we noticed a significant reduction in NAMPT activity. Similarly, the sirtuin activity changes were in agreement with the NAMPT activity changes. The lesser the NAMPT activity, the lesser the NAD^+ that was available for biological activity of Sirt-1. The plausible mechanism of AR flux through changes in NAD^+/NADH in inactivation of Sirt-1 and increased acetylation was

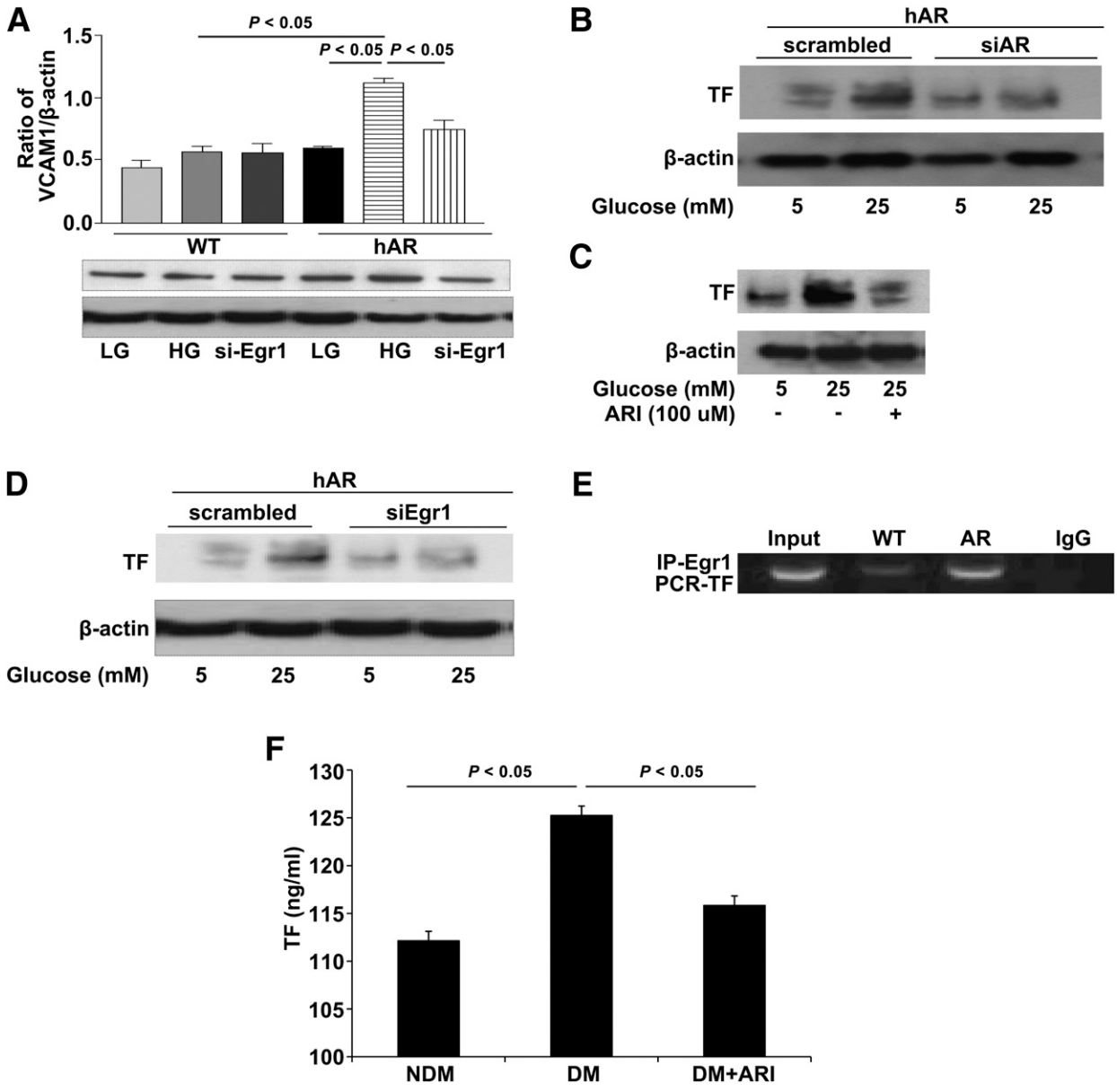

Figure 6—Expression of proinflammatory and prothrombotic markers in primary aortic endothelial cells and aortic tissues from apoE$^{-/-}$hAR mice. *A*: Expression of VCAM-1 protein in MAECs overexpressing hAR treated with 5.5 mmol/L and high glucose along with siRNA for Egr-1. The expression is represented as ratio of VCAM-1 to β-actin. Expression of TF protein was measured in MAECs overexpressing hAR, treated with siRNA for hAR (*B*), treated with 5.5 mmol/L and high glucose along with ARI (*C*), or treated with siRNA against Egr-1 under high glucose conditions (*D*). Results are expressed as ratio of TF to β-actin. *E*: ChIP was performed with anti–Egr-1 antibody in HAECs treated with high glucose to probe for promoter occupancy of Egr-1 in the TF gene. The DNA after IP was subjected to PCR using specific TF primers that include the Egr-1 binding site. The amplicons are represented in the figure. The experiments are representative of at least three independent studies. *F*: Measurement of TF by ELISA in plasma collected from apoE$^{-/-}$hAR mice with or without diabetes and diabetic mice treated with ARI. The results are expressed as nanograms per milliliter plasma ($N \geq 5$; $P < 0.05$). DM, diabetic; LG, low glucose; HG, high glucose; NDM, non-DM; siAR, siRNA for AR; si-Egr1, siRNA silencing of Egr-1.

examined. The inhibition of Sirt-1 activity was reflected by the increased acetylation of Egr-1 at 24 h of treatment with high glucose, which mediated aberrant proatherogenic signals. In our in vitro model of MAECs exposed to NMN, we could rescue the Sirt-1 activity, thereby reducing the acetylation of Egr-1. Further confirming that Egr-1 is one of the targets of Sirt-1, treatment of MAECs with a specific inhibitor, sirtinol, increased the acetylation of Egr-1. Furthermore, overexpression of Sirt-1 or pharmacological activation of Sirt-1 with SRT1720 reduced the expression of acetylated Egr-1 in HAECs exposed to high glucose. These findings confirm that Egr-1 is a potential target for NAD$^+$-dependent deacetylase Sirt-1.

Hasan et al. (30) reported that glomerular endothelial cells exposed to insulin or high concentrations of D-glucose display increased expression of Egr-1 protein and

mRNA as well as increased promoter activity. More importantly, their study suggested that moderately increased levels of glucose were sufficient to elicit Egr-1 expression irrespective of the concentration of insulin. Consistent with that study, we also report induction of Egr-1 expression at the protein, mRNA, and promoter activity levels by high glucose. We demonstrate a prolonged activation of Egr-1 in AR-expressing MAECs. Studies have reported insulin-mediated increase in Egr-1 promoter activity and cell proliferation in bovine aortic smooth muscle cells (31). However, unlike findings by us and Hasan et al., the findings of the study did not observe the effect of glucose on Egr-1. The discrepancy in results could be due to various factors but the most prominent being variation in the cell type and also the genotype. McCaffrey et al. (32) have shown increased transcripts of Egr-1 and its target genes TNF, ICAM-1, and M-CSF in human atherosclerotic lesions and in mice deficient in the LDL receptor fed high-fat diet. Studies from human atherosclerotic lesions and the mice aorta suggest predominant expression of Egr-1 in smooth muscle cells in the areas of macrophage infiltration and in endothelial cells.

Egr-1 belongs to a class of tumor suppressor genes like p53 (33). Promoters of Egr-1 have been shown to respond to Egr-1 (34). Egr-1 plays many roles in response to different stimuli; a major physiological response to increased Egr-1 levels by genotoxic stress in most cell types is apoptosis (20). In hyperglycemia, we observed an auto-feedback regulation of Egr-1 expression. ChIP studies using Egr-1 antibody showed promoter occupancy in its target gene TF. Studies in cancer cells have shown tight interrelationships between Egr-1 and other classes of similar transcription factors like p53 in transactivation and regulation of apoptosis (35). Treatment of MCF7 cells with an anticancer agent showed a sustained Egr-1 mRNA expression for 12 h (20). The initial surge of Egr-1 was attributed to early responses to stimulus; however, sustained expression was proposed to be an effect of stabilized p53 through the mouse double minute two homolog pathway (36). Other studies have shown acetylation of Egr-1 as a determinant of its own stability. The acetylation was proposed to be mediated through p300 at the consensus KDKK region in the Egr-1 protein (20). In our hypothesis, the only possibility of polyol flux mediating acetylation and stabilization of Egr-1 was through defective activity of Sirt-1 or through increased activity of p300. The latter possibility was ruled out, as our total HAT activity studies showed no significant changes between the high glucose– and the normal glucose–treated cells (Supplementary Fig. 2). Thus, to prove Sirt-1 indeed could interact with Egr-1 and deacetylate the protein, we generated mutants of the Egr-1 in which the "K" was mutated to "A." In vitro acetylation of the mutant and WT Egr-1 (KDKK) using p300 showed acetylation in the WT Egr-1 and the single mutant (ADKK) but not in the double (ADAK) or triple (ADAA) mutants of Egr-1 (Fig. 5*C*). The WT Egr-1 when subjected to in vitro deacetylation showed effective deacetylation of the acetylated Egr-1. However, a limitation of this study is the inability to infer the effect of the mutants on the TF expression, as any approach to express the mutants would not account for the already appreciable endogenous expression of the Egr-1. More solid evidence for the singular role of NAD^+ availability in limiting Sirt-1 activity was provided through our studies in HAECs, where only NMN treatment improved Sirt-1 activity and resulted in deacetylated Egr-1 and reduced TF expression.

Glucose flux via AR transiently increased Egr-1–dependent expression of procoagulant TF. Recent reports suggest that Egr-1–dependent expression of TF in smooth muscle cells exposed to free hemin, thereby leading to more vascular injury (37). Egr-1 contributes to CD-40 ligand–induced expression of TF in human endothelial cells (38). Studies in humans showed glucose-linked proinflammatory changes to increases in Egr-1, matrix metalloproteinases, and TF (39). In this context, our earlier studies have shown lesional hemorrhage in the aortic root of diabetic Tie2hAR/apoE$^{-/-}$ mice. Sirt-1 is shown to have atheroprotective effects in the vasculature by mediating vasodilation via endothelial nitric oxide (NO) synthase–derived NO and scavenging reactive oxygen species (ROS) (40). In the endothelial cells and macrophages, Sirt-1 has been shown to *1*) have anti-inflammatory functions through downregulation of expression of various cytokines through the NF-κB pathway (13), *2*) suppress macrophage foam cell formation and promote ABCA1-dependent reverse cholesterol transport, and *3*) suppress the expression of endothelial TF and exert antithrombotic properties. These findings support our data, though the stimulus remains different, and we suggest that inhibition of Sirt-1 activity through NAD^+ depletion as a consequence of AR pathway flux results in increased acetylation of Egr-1 and thereby increased expression of TF.

While we have focused on Egr-1 acetylation as a key mechanism by which AR mediates inflammation, it is also possible that impaired Sirt-1 activity–driven changes in acetylation of other transcription factors/cofactors such as forkhead box class O 1, 3, and 4; hypoxia-inducible factor-2α; and NF-κB may contribute to inflammation in our experimental settings.

While we have demonstrated a mechanism by which AR leads to acetylation of Egr-1, it is possible that AR action also mediates initial increases in unacetylated Egr-1 expression prior to its acetylation. Our earlier studies have shown that aging-linked increased flux via AR generates advanced glycation end products (AGEs): species that transduce endothelial injury consequent to their interaction with receptor of AGE (RAGE) (41). Furthermore, our group has also shown that extracellular signaling initiated by AGE-RAGE interaction regulates Egr-1 expression (42). Hence, it is conceivable that AR may induce Egr-1 increases via the AGE-RAGE axis.

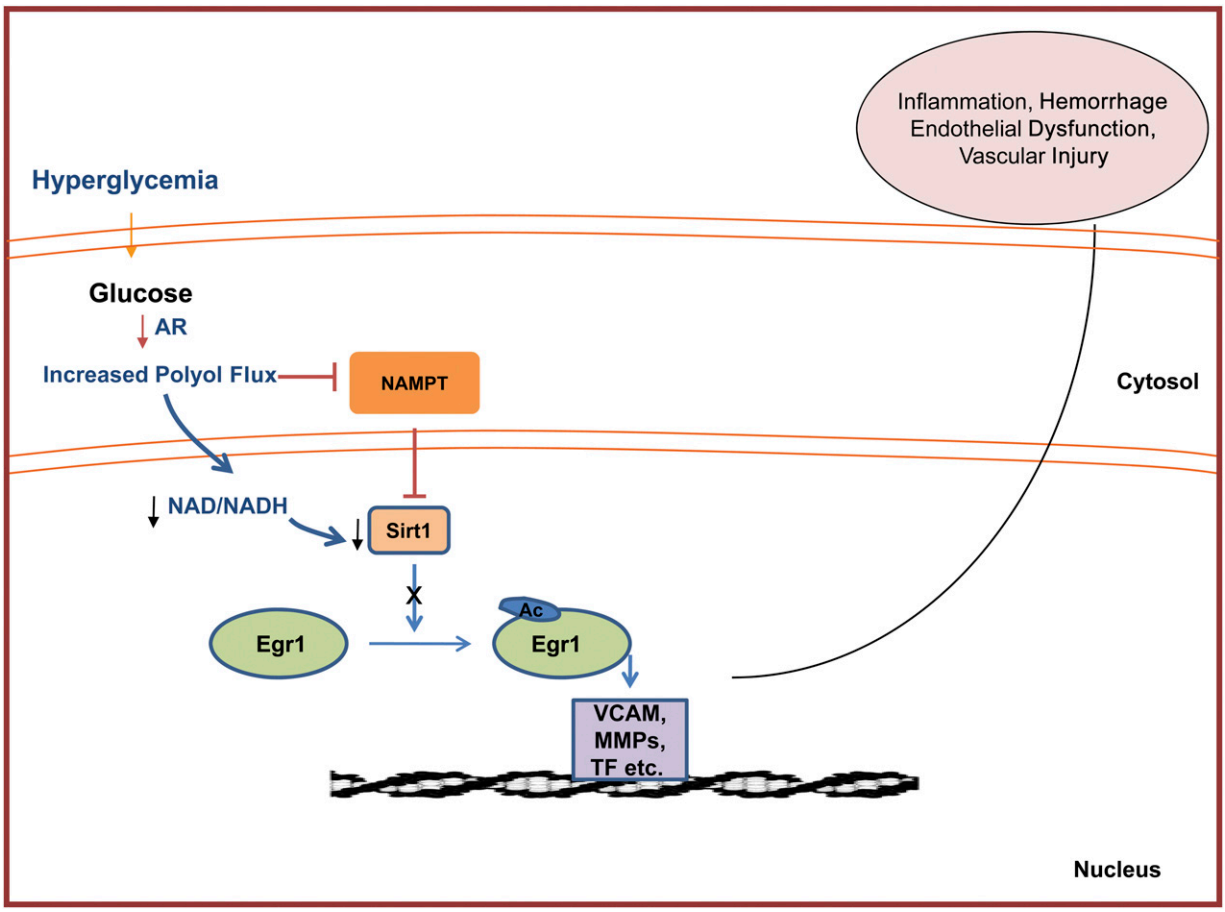

Figure 7—Scheme depicting proposed mechanism by which glucose flux via AR triggers activation, acetylation, and prolonged expression of Egr-1 leading to proinflammatory and prothrombotic responses in diabetic atherosclerosis. MMPs, matrix metalloproteinases.

Reduced lesion size and decreased inflammatory marker levels in apoE$^{-/-}$hAR^{+} mice were demonstrated upon treatment with ARI zopolresat (16). In cultured human umbilical vein endothelial cell inhibition of AR, reduced TNF-α stimulated activation of NF-kB and was linked to upregulation of ICAM-1 and VCAM-1 (43,44). Gleissner et al. (45) reported that AR gene expression and activity and ROS increases in human monocyte–derived macrophages incubated with oxidized LDL and that treatment with an ARI attenuated ROS. In support of those beneficial effects of ARI, we have provided clear evidence for improving the NAD^{+}-to-NADH ratio by enhancing the NAMPT, improving the Sirt-1 activity. In concurrence with this, we also observed reduced Egr-1 expression and TF expression in the tissues from ARI-treated diabetic apoE$^{-/-}$hAR mice.

In conclusion, we surmise that glucose flux via AR in hyperglycemia mediates atherosclerosis, in part, by influencing NAMPT-mediated NAD^{+} biosynthesis. Alteration in NAD^{+} levels causes inactivation of Sirt-1, which leads to acetylation and sustained expression of Egr-1. This, in turn, leads to increased proinflammatory and procoagulatory markers. Blockade of AR improves the NAD^{+} levels by rescuing the NAMPT biosynthesis pathway, improving Sirt-1 activity–mediated deacetylation of Egr, and subsequent induction of Egr-1 target genes during hyperglycemia (Fig. 7). Our data provide insights into novel mechanisms linking the AR pathway to the NAD^{+}/NAMPT/Sirt-1 axis in the regulation of inflammatory genes in diabetic atherosclerosis.

Acknowledgments. The authors gratefully acknowledge Latoya Woods (Diabetes Research Program, New York University Langone Medical Center) for helping in the preparation of the manuscript.

Funding. The studies were supported, in part, by grants from the National Institutes of Health (HL60901, AG026467, HL102022, and RO1 HL61783) and by the JDRF.

Duality of Interest. No potential conflicts of interest relevant to this article were reported.

Author Contributions. S.V., D.T., and R.A. assisted with the design, performed the experiments, analyzed data, and assisted with preparation of the manuscript. L.W. assisted with key experimental studies and analyzed data. R.Ro. assisted with performing animal studies. Y.S.Z. assisted with performing tissue pathology studies. I.G. and S.F.Y. provided key reagents and assisted with interpretation of data. A.M.S. provided key reagents and assisted with

study design, interpretation of data, and preparation of the manuscript. R.Ra. proposed the hypothesis, designed the studies, interpreted data, and prepared the manuscript. R.Ra. is the guarantor of this work and, as such, had full access to all the data in the study and takes responsibility for the integrity of the data and the accuracy of the data analysis.

References

1. Shukla V, Vaissière T, Herceg Z. Histone acetylation and chromatin signature in stem cell identity and cancer. Mutat Res 2008;637:1–15
2. Campos EI, Reinberg D. Histones: annotating chromatin. Annu Rev Genet 2009;43:559–599
3. Choudhary C, Kumar C, Gnad F, et al. Lysine acetylation targets protein complexes and co-regulates major cellular functions. Science 2009;325:834–840
4. Wang Q, Zhang Y, Yang C, et al. Acetylation of metabolic enzymes coordinates carbon source utilization and metabolic flux. Science 2010;327:1004–1007
5. Zhao S, Xu W, Jiang W, et al. Regulation of cellular metabolism by protein lysine acetylation. Science 2010;327:1000–1004
6. Imai S, Armstrong CM, Kaeberlein M, Guarente L. Transcriptional silencing and longevity protein Sir2 is an NAD-dependent histone deacetylase. Nature 2000;403:795–800
7. Guarente L. Sir2 links chromatin silencing, metabolism, and aging. Genes Dev 2000;14:1021–1026
8. Cheng HL, Mostoslavsky R, Saito S, et al. Developmental defects and p53 hyperacetylation in Sir2 homolog (SIRT1)-deficient mice. Proc Natl Acad Sci USA 2003;100:10794–10799
9. Luo J, Nikolaev AY, Imai S, et al. Negative control of p53 by Sir2alpha promotes cell survival under stress. Cell 2001;107:137–148
10. Daitoku H, Hatta M, Matsuzaki H, et al. Silent information regulator 2 potentiates Foxo1-mediated transcription through its deacetylase activity. Proc Natl Acad Sci USA 2004;101:10042–10047
11. Picard F, Kurtev M, Chung N, et al. Sirt1 promotes fat mobilization in white adipocytes by repressing PPAR-gamma. Nature 2004;429:771–776
12. Rothgiesser KM, Erener S, Waibel S, Lüscher B, Hottiger MO. SIRT2 regulates NF-κB dependent gene expression through deacetylation of p65 Lys310. J Cell Sci 2010;123:4251–4258
13. Breitenstein A, Stein S, Holy EW, et al. Sirt1 inhibition promotes in vivo arterial thrombosis and tissue factor expression in stimulated cells. Cardiovasc Res 2011;89:464–472
14. Rodgers JT, Lerin C, Haas W, Gygi SP, Spiegelman BM, Puigserver P. Nutrient control of glucose homeostasis through a complex of PGC-1alpha and SIRT1. Nature 2005;434:113–118
15. Vikramadithyan RK, Hu Y, Noh HL, et al. Human aldose reductase expression accelerates diabetic atherosclerosis in transgenic mice. J Clin Invest 2005;115:2434–2443
16. Vedantham S, Noh H, Ananthakrishnan R, et al. Human aldose reductase expression accelerates atherosclerosis in diabetic apolipoprotein E-/- mice. Arterioscler Thromb Vasc Biol 2011;31:1805–1813
17. Williamson JR, Chang K, Frangos M, et al. Hyperglycemic pseudohypoxia and diabetic complications. Diabetes 1993;42:801–813
18. Yamaoka T, Nishimura C, Yamashita K, et al. Acute onset of diabetic pathological changes in transgenic mice with human aldose reductase cDNA. Diabetologia 1995;38:255–261
19. Kobayashi M, Inoue K, Warabi E, Minami T, Kodama T. A simple method of isolating mouse aortic endothelial cells. J Atheroscler Thromb 2005;12:138–142
20. Yu J, de Belle I, Liang H, Adamson ED. Coactivating factors p300 and CBP are transcriptionally crossregulated by Egr-1 in prostate cells, leading to divergent responses. Mol Cell 2004;15:83–94
21. Gupta MP, Samant SA, Smith SH, Shroff SG. HDAC4 and PCAF bind to cardiac sarcomeres and play a role in regulating myofilament contractile activity. J Biol Chem 2008;283:10135–10146
22. Nishikawa T, Edelstein D, Du XL, et al. Normalizing mitochondrial superoxide production blocks three pathways of hyperglycaemic damage. Nature 2000;404:787–790
23. Brownlee M. Biochemistry and molecular cell biology of diabetic complications. Nature 2001;414:813–820
24. Cheng HM, González RG. The effect of high glucose and oxidative stress on lens metabolism, aldose reductase, and senile cataractogenesis. Metabolism 1986;35(Suppl. 1):10–14
25. Ishii H, Tada H, Isogai S. An aldose reductase inhibitor prevents glucose-induced increase in transforming growth factor-beta and protein kinase C activity in cultured mesangial cells. Diabetologia 1998;41:362–364
26. Koya D, King GL. Protein kinase C activation and the development of diabetic complications. Diabetes 1998;47:859–866
27. Wendt T, Bucciarelli L, Qu W, et al. Receptor for advanced glycation endproducts (RAGE) and vascular inflammation: insights into the pathogenesis of macrovascular complications in diabetes. Curr Atheroscler Rep 2002;4:228–237
28. Imai S, Guarente L. Ten years of NAD-dependent SIR2 family deacetylases: implications for metabolic diseases. Trends Pharmacol Sci 2010;31:212–220
29. Yoshino J, Mills KF, Yoon MJ, Imai S. Nicotinamide mononucleotide, a key NAD(+) intermediate, treats the pathophysiology of diet- and age-induced diabetes in mice. Cell Metab 2011;14:528–536
30. Hasan RN, Phukan S, Harada S. Differential regulation of early growth response gene-1 expression by insulin and glucose in vascular endothelial cells. Arterioscler Thromb Vasc Biol 2003;23:988–993
31. Gousseva N, Kugathasan K, Chesterman CN, Khachigian LM. Early growth response factor-1 mediates insulin-inducible vascular endothelial cell proliferation and regrowth after injury. J Cell Biochem 2001;81:523–534
32. McCaffrey TA, Fu C, Du B, et al. High-level expression of Egr-1 and Egr-1-inducible genes in mouse and human atherosclerosis. J Clin Invest 2000;105:653–662
33. Ahmed MM, Venkatasubbarao K, Fruitwala SM, et al. EGR-1 induction is required for maximal radiosensitivity in A375-C6 melanoma cells. J Biol Chem 1996;271:29231–29237
34. Wang B, Chen J, Santiago FS, et al. Phosphorylation and acetylation of histone H3 and autoregulation by early growth response 1 mediate interleukin 1beta induction of early growth response 1 transcription. Arterioscler Thromb Vasc Biol 2010;30:536–545
35. Ahmed MM, Sells SF, Venkatasubbarao K, et al. Ionizing radiation-inducible apoptosis in the absence of p53 linked to transcription factor EGR-1. J Biol Chem 1997;272:33056–33061
36. Calogero A, Arcella A, De Gregorio G, et al. The early growth response gene EGR-1 behaves as a suppressor gene that is down-regulated independent of ARF/Mdm2 but not p53 alterations in fresh human gliomas. Clin Cancer Res 2001;7:2788–2796
37. Hasan RN, Schafer AI. Hemin upregulates Egr-1 expression in vascular smooth muscle cells via reactive oxygen species ERK-1/2-Elk-1 and NF-kappaB. Circ Res 2008;102:42–50
38. Bavendiek U, Libby P, Kilbride M, Reynolds R, Mackman N, Schönbeck U. Induction of tissue factor expression in human endothelial cells by CD40

ligand is mediated via activator protein 1, nuclear factor kappa B, and Egr-1. J Biol Chem 2002;277:25032–25039

39. Aljada A, Ghanim H, Mohanty P, Syed T, Bandyopadhyay A, Dandona P. Glucose intake induces an increase in activator protein 1 and early growth response 1 binding activities, in the expression of tissue factor and matrix metalloproteinase in mononuclear cells, and in plasma tissue factor and matrix metalloproteinase concentrations. Am J Clin Nutr 2004;80:51–57
40. Stein S, Matter CM. Protective roles of SIRT1 in atherosclerosis. Cell Cycle 2011;10:640–647
41. Hallam KM, Li Q, Ananthakrishnan R, et al. Aldose reductase and AGE-RAGE pathways: central roles in the pathogenesis of vascular dysfunction in aging rats. Aging Cell 2010;9:776–784
42. Xu Y, Toure F, Qu W, et al. Advanced glycation end product (AGE)-receptor for AGE (RAGE) signaling and up-regulation of Egr-1 in hypoxic macrophages. J Biol Chem 2010;285:23233–23240
43. Tesfamariam B, Palacino JJ, Weisbrod RM, Cohen RA. Aldose reductase inhibition restores endothelial cell function in diabetic rabbit aorta. J Cardiovasc Pharmacol 1993;21:205–211
44. Ramana KV, Bhatnagar A, Srivastava SK. Inhibition of aldose reductase attenuates TNF-alpha-induced expression of adhesion molecules in endothelial cells. FASEB J 2004;18:1209–1218
45. Gleissner CA, Sanders JM, Nadler J, Ley K. Upregulation of aldose reductase during foam cell formation as possible link among diabetes, hyperlipidemia, and atherosclerosis. Arterioscler Thromb Vasc Biol 2008; 28:1137–1143